Journal of
Applied Remote Sensing

Ocean color patterns help to predict depth of optical layers in stratified coastal waters

Martín A. Montes-Hugo
Alan Weidemann
Richard Gould
Robert Arnone
James H. Churnside
Ewa Jaroz

SPIE

REPORT DOCUMENTATION PAGE

Form Approved
OMB No. 0704-0188

PLEASE DO NOT RETURN YOUR FORM TO THE ABOVE ORGANIZATION.

1. REPORT DATE *(DD-MM-YYYY)*	2. REPORT TYPE	3. DATES COVERED *(From - To)*
20-12-2011	Journal Article	

4. TITLE AND SUBTITLE

Ocean Color Patterns Help to Predict Depth of Optical Layers in Stratified Waters

5a. CONTRACT NUMBER

5b. GRANT NUMBER

5c. PROGRAM ELEMENT NUMBER

0601153N

6. AUTHOR(S)

Martin Montes, Alan Weidemann, Richard Gould, Robert Arnone, J. Churnside, Ewa Jarosz

5d. PROJECT NUMBER

5e. TASK NUMBER

5f. WORK UNIT NUMBER

73-9857-01

7. PERFORMING ORGANIZATION NAME(S) AND ADDRESS(ES)

Naval Research Laboratory
Oceanography Division
Stennis Space Center, MS 39529-5004

8. PERFORMING ORGANIZATION REPORT NUMBER

NRL/JA/7330-10-0555

9. SPONSORING/MONITORING AGENCY NAME(S) AND ADDRESS(ES)

Office of Naval Research
800 N. Quincy St.
Arlington, VA 22217-5660

10. SPONSOR/MONITOR'S ACRONYM(S)

ONR

11. SPONSOR/MONITOR'S REPORT NUMBER(S)

12. DISTRIBUTION/AVAILABILITY STATEMENT

Approved for public release, distribution is unlimited.

13. SUPPLEMENTARY NOTES

20120113180

14. ABSTRACT

Subsurface optical layers distributed at two different depths were investigated in Monterrey Bay, East Sound, and the Black Sea based on spatial statistics of remote sensing reflectance (Rrs). The main objective of this study was to evaluate the use of Rrs(443)/Rrs(490) (hereafter R1) skewness (ψ) as an indicator of vertical optical structure in different marine regions. Measurements of inherent optical properties were obtained using a remotely operated towed vehicle and R1 was theoretically derived from optical profiles. Although the broad range of trophic status and water stratification, a common statistical pattern consisting of lower ψR1—a deeper optical layer was found in all study cases. This variation was attributed to optical changes above the opticline and related to horizontal variability of particulates and spectral variations with depth. We recommend more comparisons in stratified coastal waters with different phytoplankton communities before the use of ψR1 can be generalized as a noninvasive optical proxy for screening depth changes on subsurface optical layers.

15. SUBJECT TERMS

ocean color, vertical structure, coastal waters, remote sensing reflectance

16. SECURITY CLASSIFICATION OF:			17. LIMITATION OF ABSTRACT	18. NUMBER OF PAGES	19a. NAME OF RESPONSIBLE PERSON
a. REPORT	b. ABSTRACT	c. THIS PAGE			Alan Weidemann
Unclassified	Unclassified	Unclassified	UL	7	19b. TELEPHONE NUMBER *(Include area code)* 228-688-6232

Ocean color patterns help to predict depth of optical layers in stratified coastal waters

Martín A. Montes-Hugo,[a] Alan Weidemann,[b] Richard Gould,[b] Robert Arnone,[b] James H. Churnside,[c] and Ewa Jaroz[b]

[a] Mississippi State University, Geosystems Research Institute, Starkville, Mississippi 39529
mmontes@gri.msstate.edu

[b] NASA, Stennis Space Center, Naval Research Lab, Hancock, Mississippi 39529
alan.weidemann@nrlssc.navy.mil; Rick.Gould@nrlssc.navy.mil;
Bob.Arnone@nrlssc.navy.mil; ewa.jarosz@nrlssc.navy.mil

[c] NOAA, Earth System Research Laboratory, Boulder, Colorado 80305
James.H.Churnside@noaa.gov

Abstract. Subsurface optical layers distributed at two different depths were investigated in Monterrey Bay, East Sound, and the Black Sea based on spatial statistics of remote sensing reflectance (R_{rs}). The main objective of this study was to evaluate the use of $R_{rs}(443)/R_{rs}(490)$ (hereafter $R1$) skewness (ψ) as an indicator of vertical optical structure in different marine regions. Measurements of inherent optical properties were obtained using a remotely operated towed vehicle and $R1$ was theoretically derived from optical profiles. Although the broad range of trophic status and water stratification, a common statistical pattern consisting of lower $\psi R1$—a deeper optical layer was found in all study cases. This variation was attributed to optical changes above the opticline and related to horizontal variability of particulates and spectral variations with depth. We recommend more comparisons in stratified coastal waters with different phytoplankton communities before the use of $\psi R1$ can be generalized as a noninvasive optical proxy for screening depth changes on subsurface optical layers.
 [DOI: 10.1117/1.3634055]

Keywords: ocean color; vertical structure; coastal waters; remote sensing reflectance; spatial statistics; thin layers.

Paper 10199RR received Dec. 20, 2010; revised manuscript received Aug. 10, 2011; accepted for publication Aug. 18, 2011; published online Sep. 2, 2011.

1 Introduction

A common assumption of remote sensing algorithms based on ocean color sensors is the vertical homogeneity of the water column in terms of optical properties. This approximation is very often not met in coastal and oceanic stratified waters due to the presence of laminar features altering the underwater light field. These submerged layers commonly correspond with thin layers (i.e., <3 m thick), have typically high concentration of dissolved and particulate material with respect to the surrounding medium, and are preferentially developed along the horizontal component.[1] Technologies used to detect vertical location of subsurface optical layers are generally based on lidar (light and range detection) systems.[1–3] Unlike these investigations, in a recent contribution we showed a new approach to discriminate waters with shallow versus deep optical layers based on passive optical measurements.[4] Briefly, the relative distance of the optical layer to the sea surface is estimated by calculating the third moment around the mean (i.e., skewness or ψ) of a specific remote sensing reflectance ratio [$R1 = R_{rs}(443)/R_{rs}(490)$]. As $\psi R1$ decreases the subsurface optical layer becomes deeper.

1931-3195/2011/$25.00 © 2011 SPIE

The present study has four objectives. First, it will test optical relationships previously found by Ref. 4 by using an alternative approach consisting of independent calculations of $\psi R1$ based on *in situ* measurements of inherent optical properties (IOPs) obtained with an undulating remotely operated towed vehicle (ROTV). Second, it will examine whether the aforementioned approach can be generalized across different marine coastal domains located at different latitudes and characterized by different trophic status. Third, it will investigate the mechanisms explaining $\psi R1$ changes in terms of IOP modifications. Finally, it will quantify the influence of water stratification on biological "layering" and its impact on $\psi R1$ patterns.

2 Methods

2.1 ROTV Surveys

High vertical resolution profiles (0.02 to 0.56 m) of *in situ* optical (i.e., total absorption coefficient of dissolved + particulate matter, a, and beam attenuation coefficient, c) and conductivity-temperature-depth (CTD) measurements were obtained using a ROTV (Scanfish MK II, intelligent undulating vehicle, EIVA, Denmark) in coastal oligotrophic [Black Sea (BS), 41.22°N to 43.70°N, 28.90°E to 31.26°E], mesotrophic [Monterrey Bay (MB), 36.33°N to 36.83°N, 121.05°W to 122.85°W], and eutrophic [East Sound (ES), 48.62°N to 48.67°N, 122.86°W to 122.89°W) waters during August to September 2008, June 2008, and May 2009, respectively. The ROTV can provide higher temporal (up to 10-fold) and spatial (up to 25-fold vertical, up to 10-fold horizontal) resolved cross sections than oceanographic gliders (e.g., electric Slocum). Thus, and given our future interest in implementing a satellite-derived approach for detecting depth of optical marine layers, we chose Scanfish as the sampling tool in this investigation.

The ROTV (0.9 × 0.3 × 1.8 m, length, height, width) was operated using an undulating mode complemented with a winch to expand the vertical sampling range up to 400 m. The ROTV has a weight of 75 kg and a payload of approximately 50 Kg. ROTV data were collected between 14 and 16 p.m. (local time) and two case studies were selected per study site: "shallow" (NS) and "deep" (FS) subsurface optical layer.

2.2 Analysis of Optical and CTD Profiles

Raw a and c coefficients were derived from an ac-9 (WetLabs) at three wavelengths (440, 488, and 675 nm) and corrected by salinity and temperature effects[5,6] using CTD (SeaBird 911) measurements. Scattering residuals were removed.[7] Only descending dives including ROTV-derived IOPs, temperature, and conductivity were processed and smoothed every 1 m along the vertical. Salinity and seawater density at each depth was derived from CTD variables and using the standard UNESCO polynomial equation of state.[8,9] For each variable, data gaps were removed by linear interpolation. Missing determinations were more common at finer spatial sampling frequencies (e.g., in ES). The pycnocline depth was defined as the depth at which vertical changes of water density were above 0.015 Kg m^{-4}.

2.3 Modeling of Ocean Color

Spectral remote sensing reflectance [$R_{rs}(\lambda)$] was estimated for each descending profile based on vertical distribution of a and c values at specific wavelengths. A light propagation model (Hydrolight, Sequoia Inc.) and ancillary data provided from airport-based meteorological stations (Black Sea, www.infospace.ru, Monterrey and Eastsound, www.wunderground.com) were used to simulate $R_{rs}(440)$ and $R_{rs}(488)$ above each Scanfish profile. For each case study, we computed the skewness of $R_{rs}(440)/R_{rs}(488)$ ratios[4] and its uncertainty by creating synthetic Scanfish transects with the same horizontal length (i.e., $n = 10$), but using different combinations

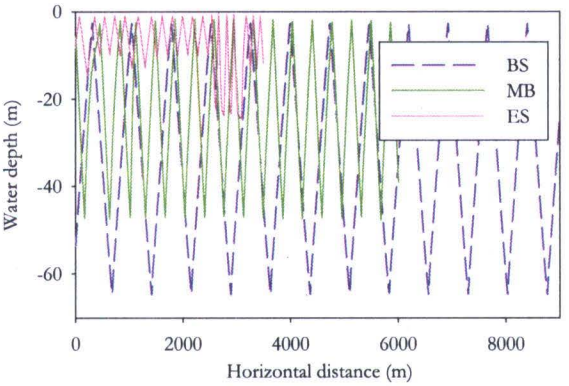

Fig. 1 An example of Scanfish MK II dives (ups and downs) in the BS, MB, and ES. BS, MB and ES sampling locations had an averaged bottom depth of 125, 120, and 27 m, respectively.

of dives (ups and downs) obtained randomly from the original datasets. For each experiment, we examined how the skewness of $R_{rs}(440)/R_{rs}(488)$ ratios and optical properties measured above the subsurface layer [e.g., $a(675)$] were interrelated. Also, we explored mechanisms behind these statistical relationships by analyzing the response of $\psi R1$ to magnitude changes on a and total scattering (i.e., $b = c - a$) coefficients at different wavelengths.

Finally, we investigated the depth of the signal source based on first optical depth (FOD) estimates. FOD was calculated as the inverse of $K_d(488)$ or the diffuse attenuation coefficient of downwelling irradiance, with $K_d(488) \sim a(488)/\tilde{\mu}$ (Ref. 10), where $\tilde{\mu}$ is the average cosine of the zenith angle of refracted solar photons (direct beam) just beneath the sea surface.

3 Results and Discussion

The ROTV diving "saw tooth" pattern varied between studied areas (Fig. 1). Depth range, averaged vertical resolution, and horizontal spacing between profiles were 2.8 to 65, 0.41, and 370.9 m for BS, 1.6 to 48, 0.36, and 268.5 m for MB, and 0.7 to 22, 0.02, and 87.4 m for ES, respectively. Cross-sections of $a(675)$ suggested that phytoplankton was an important optical component in all subsurface layers under investigation (Fig. 2). Consistent with an increase of solar radiation and freshwater river discharge as the spring–summer season progresses, the pycnocline and the optical subsurface layer characterized by relatively high $a(675)$ with respect to background (up to 3-fold) were always deeper during the second experiment in chronological order. This variation was remarkable in BS, where the vertical position of maximum $a(675)$ and pycnocline was 14 and 8.8 m in NS, and 28 and 23.2 m in FS, respectively. In general, drastic vertical changes of $a(675)$ were observed in the vicinity of the pycnocline but during the FS experiment in ES [Fig. 2(f)]. In this case, it is suggested that phytoplankton communities were not actively growing and were probably sinking as part of a post-bloom stage mainly composed of senescent cells (personal communication Dr. Percy Donaghay). Despite these differences, spatial patterns of ocean color above the sea surface always reflected similar modifications when optical submarine layering became deeper. In general, we found in every experiment that skewness of $R1$ switched from positive to negative, as the optical submarine layer was placed farther away from the sea surface (Fig. 2). Based on two standard errors [i.e., ~95 probability of rejecting null hypothesis $\mu_1 = \mu_2$, where μ is the arithmetic average, and subscript 1 and 2 refer to $\psi R1$(NS) and $\psi R1$(FS), respectively], we estimated the uncertainty of $\psi R1$ for each case study and found that a minimum of 15, 5, and 103 profiles are needed to differentiate shallow from "deeper" layers in Black Sea, Monterrey Bay, and East Sound, respectively. The size of these ideal datasets varied between 1.3 km (e.g., Monterrey Bay) and 9 km (e.g., East Sound).

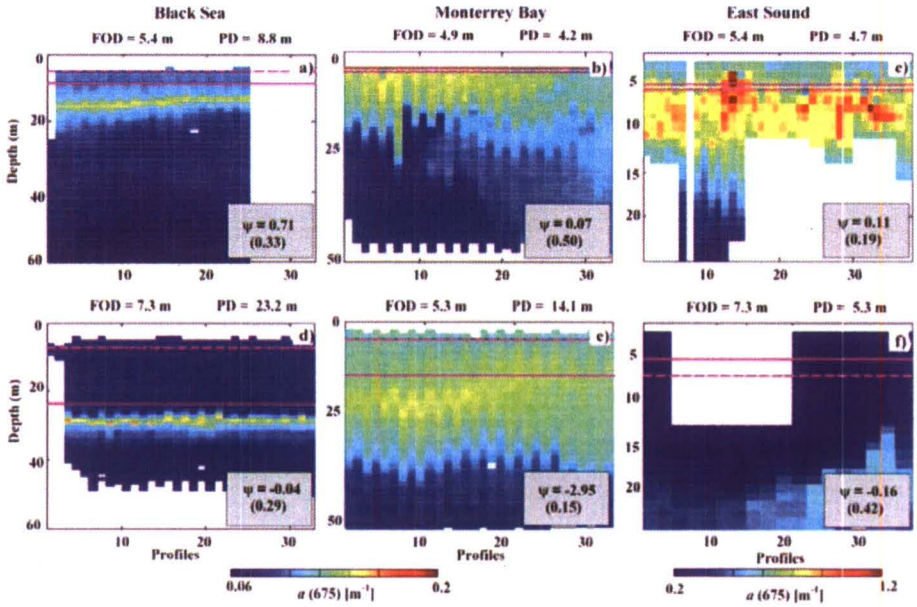

Fig. 2 Vertical position of subsurface optical layers and spatial patterns of R_{rs}. Depth variations of $a(675)$ for shallow [(a)–(c)] and deep [(d)–(f)] case studies are indicated for Black Sea [(a) and (d)], Monterrey Bay [(b) and (e)], and East Sound [(c) and (f)]. $\psi R1$ is a dimensionless variable defining the spatial skewness of $R_{rs}(443)/R_{rs}(490)$ (lower-right corner in each panel), two standard errors of $\psi R1$ are indicated between parentheses, FOD is the first optical depth in m (black dashed line), PD is the pycnocline depth in m (black solid line). Missing data are depicted in white. Plots are based on 1-m vertically averaged $a(675)$ data interpolated between Scanfish dives.

Given the relatively shallow detection depth [i.e., smaller than depth of subsurface $a(675)$ layer] of passive sensors in these waters, the aforementioned spatial changes in ocean color could be mostly explained by optical changes within the layer above the main "opticline." Indeed, we found that skewness of inherent optical properties measured in this layer and $R1$ may covary at specific wavelengths (Table 1). For each experiment, deepening of the subsurface optical layer and associated decrease of $\psi R1$ was always accompanied by a decrease on $a(490)/b(490)$ above the main opticline. This pattern was not observed at shorter wavelengths or using single optical variables instead of ratios. Thus, we suggest that dissolved colored components (i.e., constituents strongly absorbing in the UV-blue spectral range) had a smaller influence on $\psi R1$ variability with respect to that associated with particulates (e.g., phytoplankton cells, detritus, bacteria). Also, the above results imply that $\psi R1$ variability is largely modulated by light absorption and scattering.

The aforementioned covariability between $\psi R1$ and depth of the optical layer was also attributed to light spectral changes with depth. When layers are relatively shallow, the variance in the reflectance at the wavelength that is attenuated faster dominates the variance in the reflectance ratio. When the layer is relatively deeper, this wavelength stops varying since light is mostly attenuated in the layer nearest the sea surface. Thus, the variance in the reflectance in the other wavelength dominates the variance of the ratio. This change exhibits itself as a change of sign in the skewness of $R1$. The variance in reflectance at a given wavelength itself is driven by changes in the depth of the layer with the added issue of exponential weighting of the optical properties contributing to the reflectance. Hence, a meter of deepening contributes differently to variance than a meter of shallowing.

Thermohaline structure was usually coupled to depth changes of pigmented particulates as inferred from $a(675)$ (Fig. 3). These results emphasize the importance of stratification on

Table 1 Spatial statistics of opticals properties above the main opticline. For each case study, spatial skewness is computed for different IOPs and wavelengths influencing skewness of $R_{rs}(440)/R_{rs}(488)$.

Optical variable	Wavelength (nm)	Experiment	NS	FS
a	440	BS	0.29	0.11
		MB	−0.28	0.69
		ES	16.8	1.55
	488	BS	1.00	−0.02
		MB	−0.91	0.69
		ES	1.61	1.85
b	440	BS	0.42	−0.27
		MB	−0.14	0.74
		ES	0.02	0.11
	488	BS	0.29	−0.20
		MB	−0.11	0.79
		ES	0.19	2.15
b/*a*	440	BS	0.64	−0.32
		MB	−0.32	0.26
		ES	−1.47	−0.52
a/*b*	490	BS	2.50	0.28
		MB	0.69	$-8\ 10^{-5}$
		ES	1.98	0.75

vertical distribution of phytoplankton, and are consistent with other studies highlighting the major association (i.e., >70% of cases) between the depth distribution of optical layers and water column stability.[11] Despite this overall correspondence, decoupling between optical, biological, and physical variables may occur (e.g., ES in Fig. 2) when optical constituents do not behave as passive tracers (e.g., migrant phytoplankton), or they form aggregates that escape the pycnocline barrier. These ecological scenarios may introduce large uncertainties when vertical localization of submarine optical layers is based on hydrographic profiles.[12] Conversely, $\psi R1$ was very sensitive to vertical changes of subsurface optical layers for a broad range of vertical mixing and ecological conditions. However, we recommend more comparisons in stratified coastal waters with different phytoplankton communities before the use of $\psi R1$ can be generalized as a noninvasive optical proxy for screening depth changes on subsurface optical layers.

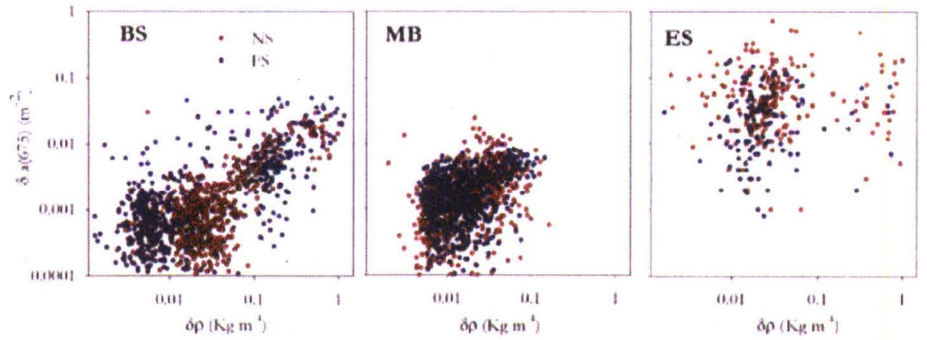

Fig. 3 Biological versus physical mechanisms modulating vertical distribution of optical properties. Vertical variation (δ) of $a(675)$ and seawater density (ρ) per meter is plotted in log10 scale. Each data point corresponds to the arithmetic average within 1 m bin. Ascending and descending Scanfish measurements are included.

Acknowledgments

We appreciate the valuable scientific comments given by Dr. Emmanuel Boss that helped to improve the original manuscript version. This work was supported by the NRL internal project "3D Remote Sensing with a Multiple-Band Active and Passive System: Theoretical Basis," PE0601153N.

References

1. J. H. Churnside and P. Donaghay, "Thin scattering layers observed by airborne lidar," *ICES J. Mar. Sci.* **66**, 778–789 (2009).
2. F. E. Hoge, W. Wright, W. B. Krabill, R. R. Buntzen, G. D. Gilbert, R. N. Swift, J. K. Yungel, and R. E. Berry, "Airborne lidar detection of subsurface oceanic scattering layers," *Appl. Opt.* **27**, 3969–3977 (1988).
3. R. Barbini, F. Colao, R. Fantoni, G. M. Ferrari, A. Lai, and A. Palucci, "Application of a lidar fluorosensor system to the continuous and remote monitoring of the Southern Ocean and Antarctic Ross Sea: Results collected during the XIII and XV Italian Oceanographic campaigns," *Int. J. Remote Sens.* **24**, 3191–3204 (2003).
4. M. Montes-Hugo, J. H. Churnside, R. W. Gould, R. A. Arnone, and R. Foy, "Spatial coherence between remotely sensed ocean color data and vertical distribution of lidar backscattering in coastal stratified waters," *Remote Sens. Environ.* **114**, 2584–2593 (2010).
5. W. S. Pegau, D. Gray, and J. R. V. Zanaveld, "Absorption and attenuation of visible and near-infrared light in water: Dependence on temperature and salinity," *Appl. Opt.* **36**, 6035–6046 (1997).
6. V. S. Langford, A. J. McKinley, and T. I. Quickenden, "Temperature dependence of the visible–near infrared absorption spectrum of liquid water," *J. Phys. Chem. A* **105**, 8916–8921 (2001).
7. J. R. V. Zanaveld, J. C. Kitchen, and C. C. Moore, "Scattering error correction of reflecting tube absorption meters," *Proc. SPIE* **2258**, 44–55 (1994).
8. F. J. Millero, C. T. Chen, A. Bradshaw, and K. Schleicher, "A new high pressure equation of state for seawater," *Deep-Sea Res.* **27A**, 255–264 (1980).
9. P. Fofonoff and R. C. Millard, "Algorithms for computation of fundamental properties of seawater," *UNESCO Technical papers* **44**, 53 (1983).
10. C. D. Mobley, *Light and Water: Radiative Transfer in Natural Waters*, Academic, San Diego, California (1994).
11. M. M. Dekshenieks, P. L. Donaghay, J. M. Sullivan, J. E. B. Rines, T. R. Osborn, and M. S. Twardowski, "Temporal and spatial ocurrence of thin phytoplankton layers in relation with physical processes," *Mar. Ecol.: Prog. Ser.* **223**, 61–71 (2001).
12. D. G. Zawada, R. V. Zanavell, E. Boss, W. D. Gardner, M. J. Richardson, and A. V. Mishonov, "A comparison of hydrographically and optically derived mixed layer depths," *J. Geophy. Res.* **110**, C11001 (2005).

Biographies and photographs of the authors not available.